JOURNAL OF VIROLOGY, Oct. 1992, p. 6117–6124
0022-538X/92/106117-08$02.00/0

Vol. 66, No. 10

RNA Recombination in a Coronavirus: Recombination between Viral Genomic RNA and Transfected RNA Fragments

CHING-LEN LIAO AND MICHAEL M. C. LAI*

Howard Hughes Medical Institute and Department of Microbiology, University of Southern California School of Medicine, Los Angeles, California 90033-1054

Received 10 March 1992/Accepted 29 June 1992

Mouse hepatitis virus (MHV), a coronavirus, has been shown to undergo a high frequency of RNA recombination both in tissue culture and in animal infection. So far, RNA recombination has been demonstrated only between genomic RNAs of two coinfecting viruses. To understand the mechanism of RNA recombination and to further explore the potential of RNA recombination, we studied whether recombination could occur between a replicating MHV RNA and transfected RNA fragments. We first used RNA fragments which represented the 5′ end of genomic-sense sequences of MHV RNA for transfection. By using polymerase chain reaction amplification with two specific primers, we were able to detect recombinant RNAs which incorporated the transfected fragment into the 5′ end of the viral RNA in the infected cells. Surprisingly, even the anti-genomic-sense RNA fragments complementary to the 5′ end of MHV genomic RNA could also recombine with the MHV genomic RNAs. This observation suggests that RNA recombination can occur during both positive- and negative-strand RNA synthesis. Furthermore, the recombinant RNAs could be detected in the virion released from the infected cells even after several passages of virus in tissue culture cells, indicating that these recombinant RNAs represented functional virion RNAs. The crossover sites of these recombinants were detected throughout the transfected RNA fragments. However, when an RNA fragment with a nine-nucleotide (CUUUAUAAA) deletion immediately downstream of a pentanucleotide (UCUAA) repeat sequence in the leader RNA was transfected into MHV-infected cells, most of the recombinants between this RNA and the MHV genome contained crossover sites near this pentanucleotide repeat sequence. In contrast, when exogenous RNAs with the intact nine-nucleotide sequence were used in similar experiments, the crossover sites of recombinants in viral genomic RNA could be detected at more-downstream sites. This study demonstrated that recombination can occur between replicating MHV RNAs and RNA fragments which do not replicate, suggesting the potential of RNA recombination for genetic engineering.

Coronaviruses are enveloped RNA viruses that infect many vertebrates. The genome of the prototype coronavirus, mouse hepatitis virus (MHV), consists of a single piece of nonsegmented positive-sense RNA of approximately 31 kb (22, 32), which is considerably larger than any other known viral RNA. Considering both the high error frequency of RNA-dependent RNA synthesis (11, 34) and the large size of MHV genomic RNA, this virus must have a unique mechanism of RNA synthesis in order to cope with the deleterious effects of possible errors. It has been postulated that the functional integrity of the large RNA genome of coronaviruses may depend at least in part on the ability of virus to recombine (18, 19).

Only a few positive-sense nonsegmented RNA viruses have been shown to undergo homologous RNA-RNA recombination at various frequencies. These include picornaviruses, coronaviruses, and a few plant viruses (1, 8, 15–17, 20, 24). Other viruses, such as Sindbis virus, can undergo recombination between defective interfering (DI) RNAs (36). The outcome was often recombinants with rearranged genome structures (36); thus, this type of recombination is atypical or aberrant homologous recombination (19). Additional viruses, such as bovine viral diarrhea virus, may undergo nonhomologous recombination, which involves recombination between unrelated viral and cellular RNAs, during natural viral infection of cows (31). Thus, the ability of RNA viruses to undergo homologous or nonhomologous recombination appears to be more common than previously recognized. Analysis of the genome structure of RNA viruses suggests that many of them have been derived by RNA recombination between related or unrelated viruses (for review, see reference 19). Among these viruses, MHV provides a particularly striking example of high-frequency RNA recombination. MHV has been demonstrated to undergo recombination not only in tissue culture (13, 14, 20, 24) but also in infected animals (12) at a frequency approaching 25% for the entire genome (4). It has been suggested that the high frequency of recombination might be due to the discontinuous and nonprocessive manner of RNA synthesis (24). This would result in the generation of freely dissociated nascent RNA fragments during MHV RNA replication (5, 6). These dissociated RNA transcripts could bind to different RNA templates and participate in RNA synthesis, leading to the generation of recombinant RNA (24).

To study the molecular basis of RNA-RNA recombination, it is important to study recombination events right after their occurrence and before selection during cell culture. We have previously established a sensitive assay system, using polymerase chain reaction (PCR) amplification to directly detect recombinant molecules among cytoplasmic RNAs from MHV-coinfected cells (3). This approach detected recombinant RNA molecules which might have a selective disadvantage during subsequent cell culture and thus might

* Corresponding author.

not be detected by the traditional method of isolation of recombinant viruses. This system has allowed us to kinetically study the recombination events between two different MHV strains in the absence of selection pressure (3). However, the inability to manipulate the large MHV genome has hampered further molecular studies of the recombination mechanism. In this report, we describe a system for examining the recombination events between MHV RNAs and transfected RNA fragments that represent the MHV 5′-end sequences that overcomes this problem. The demonstration of this type of recombination indicates that viral RNA can recombine with an existing RNA fragment which does not replicate, providing a paradigm for nonhomologous recombination, which involves disparate RNAs with different mechanisms of RNA synthesis. This study also suggests that recombination can result from dissociated nascent RNA transcripts. Furthermore, this system may enable us to understand the detailed molecular requirements for RNA-RNA recombination in MHV.

MATERIALS AND METHODS

Viruses and cells. The plaque-cloned A59 (30) and JHM (37) strains of MHV were used throughout this study. The viruses were propagated on DBT cells (10), a mouse astrocytoma cell line, at a low multiplicity of infection. For RNA transfection experiments, DBT or mouse L2 cells (21) were used as recipient cells.

Plasmid construction. Plasmid pDE-25 was derived from DI single-stranded RNA species E (DIssE), which is the smallest DI RNA from the JHM strain of MHV (28). This construct contains the complete DIssE sequence in the genomic sense placed downstream of the T7 polymerase promoter and was described elsewhere (25). Another plasmid containing a partial DIssE sequence in the anti-genomic sense was constructed by inserting the 0.84-kb *Acc*II-*Hin*fI fragment of pDE-25 DNA, representing the 5′-end sequence of DIssE RNA, into the *Eco*RI site of pGEM-3Zf(−) (Promega) after blunting the ends with T4 DNA polymerase. The orientation of the insert was confirmed by restriction enzyme analysis and DNA sequencing. The resulting plasmid was designated pDE-800(−) and produces an 864-nucleotide (nt) RNA transcript corresponding to the 5′ end of DIssE RNA in the anti-genomic sense. The plasmid representing the 5′-end fragment of genomic-sense RNA from MHV A59 was constructed by using MHV A59 virion RNA as a template for reverse transcription and PCR to generate a cDNA containing the 5′-end genomic-sense sequence of the A59 virion RNA. The first primer (5′-ATCCTCTACAT TAAAGTCATACACA-3′), which is complementary to nt 848 to 872 of the 5′ end of the A59 genome, was used for reverse transcription to synthesize first-strand cDNA. The second primer (5′-GAAATTAATACGACTCACTATAGG GATATAAGAGTGATTGGCGTCCGTAC-3′) contains the T7 polymerase promoter sequence at the 5′ end, followed by MHV 5′-end sequence from nt 1 to 24. This primer was used in PCR to amplify double-stranded cDNA. The PCR product, containing the A59 5′ end of the genomic-sense sequence extending from nt 1 to 872, was then cloned into the *Sma*I site of pTZ-18U (U.S. Biochemicals). The resulting plasmid was designated pA833.

RNA transcription. To generate the 5′-end genomic-sense fragments of DIssE RNA, pDE-25 DNAs were linearized by digestion with *Bam*HI (for 466-nt RNA) or *Acc*II (for 833-nt RNA), and the DNA fragments were purified from low-melting-point agarose. Linearized plasmids were transcribed with T7 RNA polymerase in the presence of a cap analog, $m^7G(5')ppp(5')G$ (New England Biolabs), as described previously (33). Similarly, pDE-800(−) was used to obtain the 5′-end anti-genomic-sense RNA fragments of DIssE RNA (864 nt in length) by *Xba*I digestion and T7 RNA polymerase transcription. Plasmid pA833 was used to synthesize MHV A59 5′-end genomic-sense RNA fragments (833 nt in length) by *Acc*II digestion and T7 RNA polymerase transcription.

RNA transfection. Confluent L2 cells or DBT cells were infected with A59 or JHM virus at a multiplicity of infection of 5. The virus- and mock-infected cells were subjected to RNA transfection at 1 h postinfection. For L2 cells, transfections were performed by the DEAE-dextran method as described previously (25). For DBT cells, transfections were performed by the Lipofectin method (GIBCO BRL). Briefly, at 1 h postinfection, monolayers of DBT cells at approximately 80% confluence in a 6-cm petri dish were washed once with serum-free Eagle's minimal essential medium (MEM) and then covered with 4 ml of warm serum-free MEM. Ten micrograms of in vitro-transcribed RNAs was dissolved in a final volume of 100 μl of 50% (vol/vol) Lipofectin. The RNA-Lipofectin mixtures were incubated at 25°C for 20 min and then added slowly to cell cultures. After incubation for 4 h at 37°C, the inoculum was removed, and cells were washed twice with warm serum-free MEM and further incubated for up to 14 h (for cells infected with strain A59) or 16 h (for cells infected with strain JHM) in the presence of MEM containing 7% newborn calf serum. Culture fluid was harvested, clarified, and stored at −80°C.

Preparation of virion RNA and intracellular viral RNA. Virion RNA was extracted from the purified viral particles by previously described procedures (3) with slight modification. Briefly, cells were infected with A59 or JHM virus. At 13 h postinfection, the medium containing released virus particles was harvested, and virions were pelleted through a 30% sucrose cushion at 26,000 rpm in a Beckman SW28 rotor for 3.5 h. Viral pellets were resuspended in NTE (100 mM NaCl, 10 mM Tris-HCl [pH 7.5], 1 mM EDTA) buffer and treated with 50 μg of RNase A (Sigma) per ml at 37°C to remove possible contaminants from cellular RNA. The mixture containing the viral genomic RNA was digested with 500 μg of proteinase K (Boehringer Mannheim Biochemica) per ml and extracted twice with phenol-chloroform. Intracellular viral RNA was isolated from MHV-infected cells by the protocol described previously (23, 28).

PCR amplification of RNAs and cDNA sequencing. Ten micrograms of intracellular viral RNA or 3 μg of virion RNA was reverse transcribed into cDNA. Briefly, the RNAs were denatured at 94°C for 2 min and incubated at 42°C for 60 min in 50 μl of reaction mixture containing 1 U of avian myeloblastosis virus reverse transcriptase (Seikagaku America Inc.), 10 mM $MgCl_2$, 100 mM KCl, 50 mM Tris-HCl (pH 8.0), a 0.1 mM concentration of each of the four deoxyribonucleoside triphosphates, and 1 μM synthetic oligonucleotide primer 1 (5′-TCGGGTTAAGATGAACCTCCTCTC-3′), which is complementary to nt 877 to 900 of the 5′ end of both A59 and JHM viral genomic RNA. The cDNAs were then used as templates for PCR amplification. Briefly, 10 μl of the reverse transcription mixture was mixed with 90 μl of PCR buffer (10 mM Tris-HCl [pH 8.3], 1.5 mM $MgCl_2$, 50 mM KCl, 1 mg of gelatin per ml) containing 2 U of *Taq* DNA polymerase (Boehringer Mannheim Biochemica), 50 μM each deoxyribonucleoside triphosphate, and 0.5 μM synthetic oligonucleotide primer 2 (5′-TGGCGTCCGTACG TACCTAA-3′), which is complementary to nt 13 to 32 of DIssE 5′-end sequences, or primer 3 (5′-TGTGCTTC

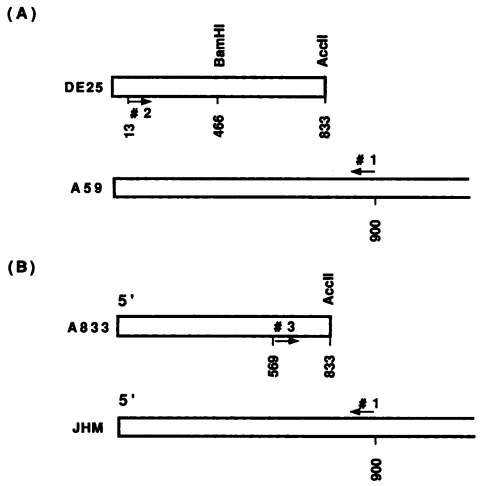

FIG. 1. Genetic locations of primers used to detect recombinant RNAs. (A) Primers 1 and 2 were used to detect DIssE head-A59 body recombinants. Primer 1 is complementary to A59 sequences from nt 877 to 900, and primer 2 is specific for DIssE sequences from nt 13 to 32. The corresponding region of A59 has a three-nucleotide divergence from the 3' end of the primer. The specificity of this primer was demonstrated previously (2). (B) Primers 1 and 3 were used to detect A59 head-JHM body recombinants. Primer 3 was specific for the A59 sequence from nt 569 to 587.

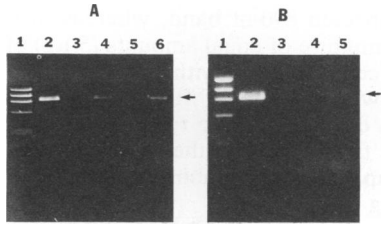

FIG. 2. PCR amplification of DIssE-A59 recombinants. (A) Recombinant RNA from intracellular RNAs. Lane 1, *Hae*III-digested φX174 size markers. Lane 2, intracellular RNA from A59-infected L2 cells amplified with primers 196 and 152 (specific for the A59 peplomer gene) (3). Lanes 3 through 6, intracellular RNAs amplified with primers 1 and 2: lane 3, mixture of equal amounts of intracellular RNA from A59-infected, mock-transfected L2 cells and from mock-infected, 833-nt-RNA-transfected L2 cells; lane 4, intracellular RNA from A59-infected, 833-nt-RNA-transfected L2 cells; lane 5, mixture of equal amounts of intracellular RNA from A59-infected, mock-transfected L2 cells and from mock-infected, 466-nt-RNA-transfected L2 cells; lane 6, intracellular RNA from A59-infected, 466-nt-RNA-transfected L2 cells. (B) Recombinant RNA from virion RNAs. Lane 1, *Hae*III-digested φX174 size markers. Lane 2, virion RNA from A59-infected L2 cells detected with primers 196 and 152, specific for the A59 S gene. Lanes 3 through 5, virion RNA amplified with primers 1 and 2: lane 3, virion RNA from mock-infected, mock-transfected L2 cells; lane 4, virion RNA from A59-infected L2 cells; lane 5, virion RNA from A59-infected, 833-nt-RNA-transfected L2 cells. The arrows indicate the specific PCR products of approximately 890 nt.

CCAAAACAGCT-3'), which is complementary to nt 569 to 587 of the 5' end of A59 RNA. Amplification was carried out for 40 cycles at 94°C for 1.5 min, 60°C (or 62°C for some experiments) for 2 min, and 72°C for 3 min per cycle. The PCR products were then subcloned into pTZ-18U or pBluescript SK(+) (Stratagene) according to the protocol described previously (2). Double-stranded plasmid DNA sequencing was performed with the Sequenase system (U.S. Biochemicals).

RESULTS

Recombination between the A59 viral genome and the transfected 5'-end RNA fragments of DIssE RNA. To study whether recombination could occur between the MHV genome and a transfected RNA fragment, we used a PCR assay system (3) to detect recombinant RNAs among the intracellular RNAs and virion RNAs. We first studied the possible recombination between the MHV A59 genome and the 5'-end genomic-sense RNA fragments of DIssE, which is a DI RNA derived from MHV JHM (26).

We first examined whether recombinant RNAs could be detected in the intracellular RNA from cells infected with A59 and transfected with the 5'-end RNA fragment of DIssE. These recombinant RNAs were detected by PCR with two synthetic primers, 1 and 2 (Fig. 1A and Materials and Methods), which are specific for A59 RNA sequences at the 3' end and for DIssE RNA at the 5' end, respectively. The region between these two primers spanned 890 nt; only recombinant RNAs which had an odd number of crossovers between these two primer sites and contained DIssE-specific sequences on the 5' side and A59-specific sequences on the 3' side (i.e., DIssE head-A59 body) could be detected by this PCR assay system. The PCR conditions (94°C for 1.5 min, 60°C for 2.0 min, and 72°C for 3 min for each cycle, 40 cycles) were chosen empirically so that these two primers would bind only to recombinant RNAs and would not generate nonspecific PCR products. The PCR products were separated by electrophoresis on a 1.2% agarose gel, and the results are shown in Fig. 2A. In lane 4 of Fig. 2A, there was a specific 890-nt band from the RNAs isolated from L2 cells infected with A59 and transfected with the 833-nt RNA fragment. In contrast, there was no specific band detected in lane 3, which represented the RNA mixture of 5 μg each of cytoplasmic RNA from A59-infected, mock-transfected cells and from mock-infected, 833-nt-RNA-transfected cells. Another control experiment for the PCR reaction (Fig. 2A, lane 2) showed that cytoplasmic RNAs from the A59-infected cells yielded the expected PCR product (870 nt long) with two specific primers, primer 196 (5'-ATATCAAGCTTGAG CACACGGGCAATAAC-3'), which is complementary to nt 1430 to 1449 from the 5' end of the peplomer gene, and primer 152 (5'-GGACTGAGCTCCGCTTAATGTTAATG GCTGATGCAT-3'), which is homologous to nt 581 to 604 of the A59 peplomer gene. Additionally, other control experiments showed that RNA from the A59-infected, mock-transfected cells did not yield any PCR products with primers 1 and 2 (data not shown). These control experiments clearly demonstrated that the 890-nt band in Fig. 2A, lane 4, was not a PCR artifact generated by transcriptional jumping of reverse transcriptase or *Taq* polymerase, but most likely represents a recombination event occurring in the infected cells. These data strongly suggest that the transfected 833-nt RNA fragment from the 5' end of the genome, which cannot replicate, was able to recombine with the A59 genomic RNAs during infection.

We also examined whether a shorter 5'-end RNA fragment could recombine with the viral genomic RNAs. L2 cells were infected with A59 and transfected with the 466-nt RNA fragment transcribed from pDE-25 linearized with *Bam*HI. The cytoplasmic RNAs were isolated as templates for reverse transcription and PCR detection with the same primers 1 and 2 described above. The result is shown in Fig. 2A, lane

6, as the expected 890-nt band, whereas in lane 5, which contained a mixture of equal amounts (5 μg) of cytoplasmic RNA from cells infected with A59 alone and from cells transfected with the 466-nt RNA only, no specific PCR product was detected. These results demonstrated that the 466-nt RNA fragment from the 5′ end of the viral genome was also capable of recombining with the A59 genomic RNAs during infection.

To further demonstrate that the PCR product formed between the viral genomic RNA and transfected RNAs represented functional recombinant RNA molecules, we studied whether the recombinant RNA could be detected in the virion RNA released from these cells. Since the RNA fragments used for transfection did not contain the packaging signal (29), they would not be packaged into virus particle. Thus, any DIssE-specific sequence in the virion was most likely derived from the replicating recombinant genomic RNA. L2 cells were infected with A59 and transfected with the 833-nt RNA fragment as described above. At 14 h postinfection, the culture medium containing released virus particles was harvested and then inoculated onto confluent DBT cells for additional passage. The supernatant from this infection, termed passage 1, was harvested, and the viral particles were purified. The purified virus particles were treated with RNase A to remove any contaminating cellular RNA, and viral genomic RNA was then isolated and subjected to reverse transcription and PCR detection with primers 1 and 2 as described above. The specific 890-nt PCR product derived from the recombinant RNA was again detected (Fig. 2B, lane 5), suggesting that recombinant RNAs between viral genomic RNAs and transfected RNA fragments represented viable recombinant virus which could replicate and could be packaged into virus particles during serial passages. This is reminiscent of recombinant viruses generated from cells coinfected with two different MHV strains (3). Appropriate controls, including virion RNAs from A59-infected, mock-transfected cells or from mock-infected cells (Fig. 2B, lanes 3 and 4), did not yield this PCR product.

Identification of the recombination sites in DIssE-A59 recombinants. To determine the crossover sites in these recombinant RNAs, the 890-nt PCR products from both the intracellular RNA and virion RNA were purified from low-melting-point agarose and subcloned into the vector pTZ-18U. DNA sequence analysis data for 53 clones of PCR products from cytoplasmic RNAs and 43 clones of PCR products from virion RNAs are summarized in Fig. 3. The vast majority of recombinants from either intracellular or virion RNAs had recombination sites somewhere upstream of the pentanucleotide repeat sequences (UCUAA) (designated R in Fig. 3); 44 of the 53 clones from intracellular RNAs and 42 of the 43 clones from virion RNAs had crossovers between nt 36 and 69. However, nine clones from intracellular RNAs and one clone from virion RNAs had crossover sites slightly downstream of the pentanucleotide repeat sequences (Fig. 3). Thus, the pentanucleotide region, which lies between the leader sequence and the genomic sequence, was a recombinational hot spot. Moreover, most clones from the intracellular RNAs and all clones from the virion RNAs contained the nine nucleotides (CUUUA UAAA) immediately downstream of the pentanucleotide repeat sequences after one passage. This sequence is deleted in DIssE RNA and most other DI RNAs (25). Only six clones from intracellular RNAs (Fig. 3) had a deletion of the nine nucleotides. This result suggests that the presence of the nine nucleotides gave a selective advantage.

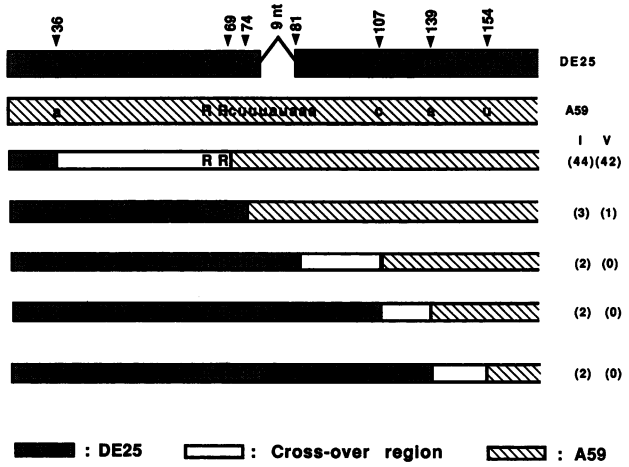

FIG. 3. Recombination sites of DIssE-A59 recombinants. DNA sequence analyses of 53 clones of PCR products from intracellular RNAs and 43 clones of PCR products from virion RNAs are summarized. The numbers and arrowheads indicate nucleotide positions of crossovers. R, pentanucleotide (UCUAA) sequences. The DIssE (DE25) RNA fragment has a 9-nt deletion downstream of the pentanucleotide repeat sequences; A59 genomic RNA contains this 9-nt sequence (CUUUAUAAA). Recombination can occur anywhere between the given positions in the crossover regions (open areas); the precise site could not be determined because the parental RNAs had identical sequences within this region. The numbers in parentheses are the number of cDNA clones from PCR products for intracellular recombinants (I) and recombinants from virion RNAs (V).

Recombination between DIssE 5′-end RNA fragments in the anti-genomic sense and the A59 genome. We next determined whether RNA fragments in the anti-genomic sense (negative polarity) could also undergo recombination with the virion RNA. L2 cells were infected with A59 and transfected with the anti-genomic-sense RNA fragment of the 5′-end 864 nt of DIssE RNA [864(−) RNAs]. Intracellular RNAs were used for reverse transcription and PCR detection of the recombinant RNAs with primers 1 and 2, which detect only recombinant RNA in the genomic sense. Interestingly, a specific 890-nt band was detected (Fig. 4, lane 6). A control experiment in which the RNA mixture contained equal amounts (5 μg) of cytoplasmic RNA from cells infected with A59 alone and from cells transfected only with 864(−) RNAs did not give this PCR product (Fig. 4, lane 5).

To rule out the possibility that the 864(−) RNA preparations were contaminated with genomic-sense RNA fragments or double-stranded DNA fragments, we examined cytoplasmic RNAs from L2 cells transfected only with 864(−) RNAs by reverse transcription and PCR with a specific pair of primers: 124, which is complementary to the MHV 5′-end sequence from nt 1 to 24 in the anti-genomic sense, and 320, which is complementary to nt 848 to 872 from the 5′ end of the A59 genome in the genomic sense. The specific PCR product could be detected when primer 124 was used in reverse transcription and primer 320 was used in PCR, but not when primer 320 was used in reverse transcription and primer 124 was used in PCR (data not shown). These results indicated that the 864(−) RNA was not contaminated with genomic-sense RNA or double-stranded DNA fragments. Thus, the PCR product detected in Fig. 4, lane 6, represented a specific recombinant RNA between A59 virion RNA and transfected 864(−) RNAs. It is note-

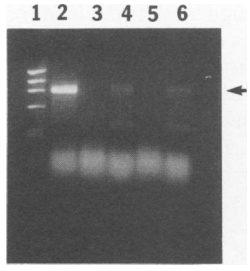

FIG. 4. PCR detection of recombinant RNA between the A59 genome and the anti-genomic-sense RNA fragment from the 5′ end of DIssE RNA. Lane 1, *Hae*III-digested ϕX174 size markers. Lane 2, intracellular RNA from A59-infected L2 cells amplified with primers 196 and 152 (specific for the A59 S gene). Lanes 3 through 6, intracellular RNAs amplified by primers 1 and 2: lane 3, mixture of equal amounts of intracellular RNA from A59-infected, mock-transfected L2 cells and from mock-infected, 833-nt-RNA-transfected L2 cells; lane 4, intracellular RNA from A59-infected, 833-nt-RNA-transfected L2 cells; lane 5, mixture of equal amounts of intracellular RNA from A59-infected, mock-transfected L2 cells and from mock-infected, 864(−) RNA-transfected L2 cells; lane 6, intracellular RNA from A59-infected, 864(−) RNA-transfected L2 cells. The arrow indicates the specific PCR products of 890 nt.

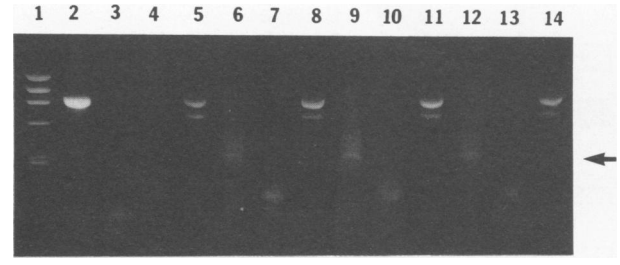

FIG. 5. PCR detection of recombinants between JHM and the 5′-end RNA fragment of A59. Lanes 2, 4, 7, 10, and 13 were amplified with primers 196 and 152, specific for the peplomer gene of A59. Lanes 3, 6, 9, and 12 were amplified with primers 1 and 3, specific for the recombinant. Lanes 5, 8, 11, and 14 were amplified with primers 1 and 124, the latter of which is complementary to nt 1 to 24 from the 5′ end of the A59 genome. Lane 1, *Hae*III-digested ϕX174 size markers. Lane 2, virion RNA from A59-infected DBT cells. Lanes 3 to 5, virion RNA from JHM-infected DBT cells. Lanes 6 to 8, virion RNA from passage 1 of the virus from cells infected with JHM and transfected with the 5′-end RNA fragment of A59. Lanes 9 to 11, virion RNA from passage 4. Lanes 12 to 14, virion RNA from passage 6. The arrow indicates the specific PCR product of approximately 330 nt in lanes 6, 9, and 12.

worthy that since the PCR primers used here could detect only genomic-sense RNA, the transfected 864(−) RNAs must have been converted into genomic-sense RNAs before they could be detected by PCR. This result suggested that the recombinant RNA had replicated in the infected cells. Since the transfected 864(−) RNAs represented the 3′ end of the negative-strand RNA of the viral genome, this transfected RNA must have been converted to the genomic-sense RNA before recombination; alternatively, recombination may have occurred by a breakage and rejoining mechanism (see Discussion).

The identity of these recombinant RNAs was further confirmed by DNA sequence analysis of the PCR products after they were cloned into the pBluescript SK(+) vector. Sequence analysis of the seven clones showed that all of them had a crossover site located between the sites for the two primers, with the 5′-end sequence being derived from DIssE and the 3′-end sequence being derived from A59 (data not shown). Six of the seven clones had a crossover site located between nt 139 and 154 from the 5′ end, whereas one clone had a crossover site at nt 69.

Recombination between A59 5′-end RNA fragments and JHM genome. To examine whether recombination could also occur between the virion RNA and the transfected RNA fragment in a reciprocal pair of RNAs, we studied the possible recombination between JHM RNA and a transfected RNA fragment from A59. The 5′-end 833-nt RNA fragment of the genomic-sense A59 RNA was transfected into JHM-infected cells. The virus released from these cells were used to infect confluent DBT cells. Viral particles released from the latter were termed passage 1 virus and were serially passaged further on DBT cells.

Viral genomic RNA from each passage was purified and analyzed by reverse transcription and PCR amplification with primers 1 and 3 (Fig. 1B), which spanned 330 nt. These two primers were chosen because these are the only regions where A59 and JHM RNA sequences are sufficiently different for adequate primer specificity. Only recombinant RNAs which had a crossover between these two primers and contained A59-specific sequences on the 5′ side and JHM-specific sequences on the 3′ side could be detected by this PCR assay procedure. The PCR conditions (94°C for 1.5 min, 62°C for 2.0 min, and 72°C for 3 min for each cycle; 40 cycles) were chosen empirically so that these two primers would bind only to recombinant RNAs and would not generate nonspecific PCR products. The results showed that virus from all passages tested yielded a PCR product specific for the recombinants. The specific PCR products (330 nt long) from passages 1, 4, and 6 are shown in Fig. 5 (lanes 6, 9, and 12, respectively). A control experiment showed that JHM virus alone did not yield this PCR product (Fig. 5, lane 3). To confirm that the JHM virus stocks were not contaminated with A59 virus, the viral genomic RNAs from the JHM stock and from different passages were screened by PCR with a pair of primers (196 and 152; see above) which were specific for the peplomer gene sequences of A59. No PCR product was detected (Fig. 5, lanes 4, 7, 10, and 13). In contrast, all of them yielded a PCR product (900 nt) with primers 1 and 124, the latter of which is complementary to nt 1 to 24 of the 5′ end of the MHV genome (Fig. 5, lanes 5, 8, 11, and 14). This product represented the JHM viral RNA. The lower band probably represented misprimed PCR products.

To analyze the crossover sites of these recombinants, the PCR products from passage 1 (Fig. 5, lane 6) and passage 6 (Fig. 5, lane 12) were subcloned into the vector pBluescript KS(+) and sequenced. Figure 6 is a summary of the DNA sequence analysis data for 33 clones from passage 1 and 13 clones from passage 6. The sequence data revealed that all clones were true recombinants, with a crossover between the sites for primers 1 and 3. In addition, in contrast to passage 1, the recombinant with a crossover between nt 587 and 609 was a dominant population in passage 6 (Fig. 6), suggesting that a certain type of recombinant viruses was selected during serial viral passages. These results indicated that recombination could occur between a viral RNA and a nonreplicating RNA fragment, resulting in functional recombinant viral RNA.

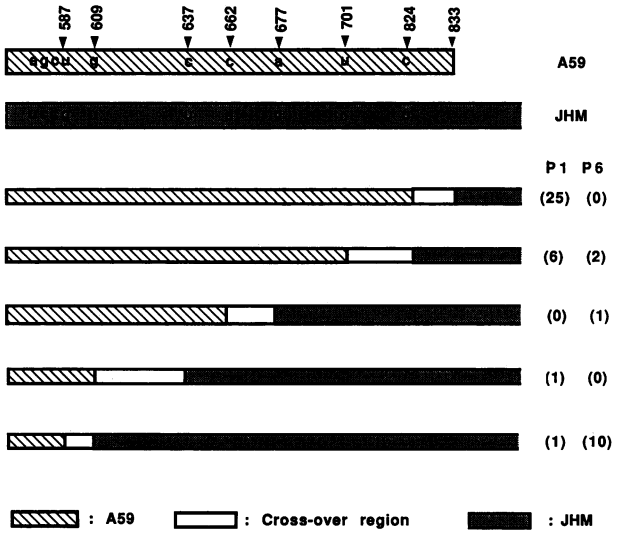

FIG. 6. Recombination sites of A59-JHM recombinants. This figure summarizes the DNA sequence analysis data for 33 clones from passage 1 (P 1) and 13 clones from passage 6 (P 6). The numbers and arrowheads indicate the positions of crossovers. Recombination can occur anywhere between the given positions in the crossover regions (open areas). The numbers in parentheses are the number of cDNA clones from PCR products after passages 1 and 6.

DISCUSSION

This study demonstrated the occurrence of recombination between viral RNAs and a transfected RNA fragment. The results suggest that an RNA fragment which cannot replicate itself can participate in RNA recombination. The ability of nonreplicating RNAs to recombine with replicating RNAs is a prerequisite for nonhomologous recombination between viral RNA and cellular RNA, since the latter is not directly involved in viral RNA replication. Thus, this system can potentially serve as a paradigm for understanding the mechanism of nonhomologous recombination. Furthermore, this system will allow the eventual determination of the structural requirements for RNA recombination because the RNA fragments can be easily manipulated. Most important, this approach allows mutation of the 5′-end RNA sequence without recourse to a full-length infectious cDNA clone, which is still not feasible for MHV because it has a 31-kb-long RNA genome (22, 32). The potential utility of such an approach was recently demonstrated by a study of recombination between a 3′-end RNA fragment and genomic RNA from MHV (17a).

The data presented in this report demonstrate that the 5′-end RNA fragments of MHV in both the genomic and anti-genomic sense are recombinogenic. All of the RNA fragments used in this study contain the leader sequences and thus are similar to the free leader-containing RNA intermediates detected in MHV-infected cells (5, 6). We have previously proposed that these leader-containing RNAs represent interrupted nascent RNA transcripts, which are dissociated from the template but may reassociate with the same or different RNAs to continue transcription (24). Thus, recombinant RNAs could result from free RNA transcripts from one virus strain binding to the RNA templates from another strain and reinitiating RNA transcription (24). The results presented in this report support such a hypothesis and strongly suggest that the leader sequence-containing RNA intermediates detected in the MHV-infected cells (5, 6) could be recombinogenic via a copy choice mechanism.

Two possible mechanisms can explain how the transfected 5′-end RNA fragments recombine with MHV RNAs (Fig. 7). Both mechanisms assume that RNA recombination occurs by a copy choice mechanism and thus occurs during the replication process. In model A (Fig. 7A), exogenous genomic-sense RNAs (e.g., DIssE RNAs) bind to the endogenous template via complementary sequences and act as primers for genomic (positive)-sense RNA synthesis. Conceivably, the replicase complex may have some proofreading activity to trim 3′-end mismatching sequences from the exogenous RNA, and the trimmed RNA fragment is then used as a primer to complete the synthesis of genomic-strand RNA. After one round of RNA replication, this would generate DIssE head-A59 body recombinants. The trimming of primer to different extents and subsequent transcription would result in recombinant RNAs with various crossover sites. Such a cleavage of RNA in the transcription complex has been demonstrated in prokaryotic cells (35). In the alternative model B (Fig. 7B), the transfected RNA fragments act as the template during negative-strand synthesis. Conceivably, the replicase complex, along with newly synthesized negative-strand transcripts, might dissociate from the original genomic template and then use the transfected RNA as a template to complete the first round of negative-strand synthesis; the subsequent genomic-strand synthesis would generate DIssE head-A59 body recombinants. Since all of the transfected RNAs used in this study contained intact leader sequences, only one crossover (switching) event was required to generate recombinants. Whether RNA fragments without the leader sequence (e.g., the central part of the MHV genome) could also recombine with virion RNAs remains to be studied. Since such RNA fragments need at least two switching events to generate a functional recombinant RNA, the efficiency of this type of recombination will be considerably lower.

It is of interest that the transfected anti-genomic sense 864(−) RNA fragment could also undergo recombination with virion RNA. All of the recombinants obtained contained a DIssE head-A59 body recombination and had a crossover between the sites for primers 1 and 2. Two mechanisms can explain the generation of these recombinants (Fig. 7C and D). (i) The negative-sense RNAs are first used as templates and transcribed into genomic-sense RNAs. This is quite feasible, since these anti-genomic-sense RNA fragments should contain signals for positive-sense RNA replication. The 5′-end positive-sense transcripts can then recombine with virion RNAs by template switching. (ii) It is conceivable that these anti-genomic-sense RNAs can recombine directly with negative-sense MHV RNA by a breakage-rejoining mechanism. Although RNA recombination is generally thought to be mediated by a copy choice mechanism (9, 17), the breakage-rejoining mechanism has never been rigorously ruled out. In fact, the genetic structure of some recombinant RNAs in plant RNA viruses is more compatible with the breakage-rejoining mechanism (7). This mechanism could allow the negative-sense MHV RNA to fuse with the transfected 864(−) RNA fragment, which corresponds to the 3′ end of the negative-sense RNA. Although we cannot distinguish between these possible mechanisms at present, the participation of both transfected positive- and negative-sense RNA fragments in recombination suggests that recombination can occur during both positive- and negative-sense RNA synthesis. It has previ-

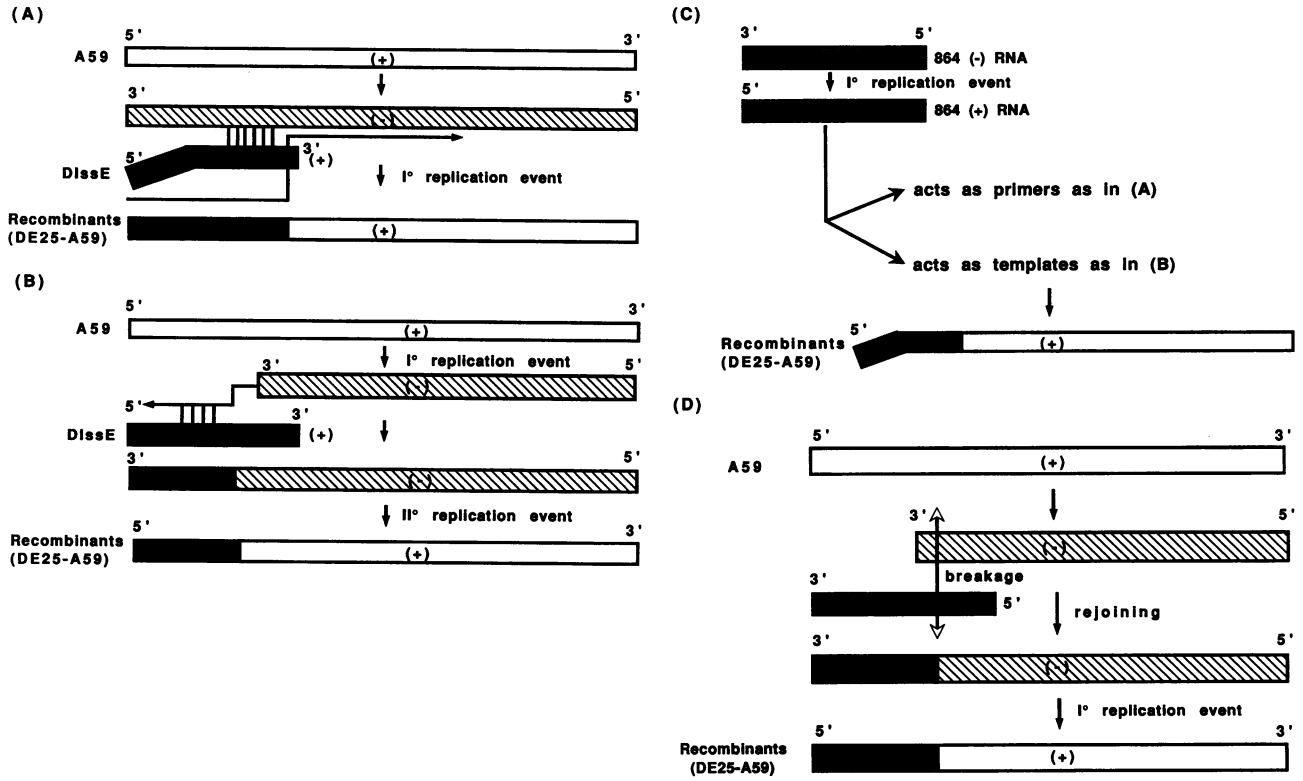

FIG. 7. Models for the mechanism of recombination between transfected RNA fragments and MHV genomic RNAs. (A) Exogenous RNAs act as primers during genomic-strand synthesis; recombinants could be obtained after one round of RNA replication. (B) Exogenous RNAs act as templates during minus-strand synthesis; recombinants could be obtained after two rounds of RNA replication. (C) Exogenous 864(−) RNA was first used as the template and transcribed into genomic-sense RNAs [864(+) RNA], which act as primers or templates in the same way as depicted in A and B, respectively. (D) 864(−) RNA molecules recombine with negative-sense MHV RNA by a hypothetical breakage-rejoining mechanism. DE25, plasmid pDE-25, representing DIssE RNA. I° and II° mean first and second, respectively.

ously been shown that poliovirus RNA recombination occurs mainly during negative-strand RNA synthesis (17). However, this apparent result could have been due to the fact that poliovirus positive-strand RNA is present in great excess over negative-strand RNA, providing a greater opportunity for template switching during negative-strand RNA synthesis. When a large amount of negative-sense RNA was transfected into cells in our study, the opportunity for template switching during positive-strand RNA synthesis could have increased proportionally. Thus, our results suggest that RNA recombination can occur during both positive- and negative-strand RNA synthesis.

The crossover sites identified in this study were distributed in many different places in every genetic cross. This is reminiscent of the recombination sites identified during MHV coinfection in the absence of selection pressure (3). However, the predominant crossover sites (hot spots) differed depending on the structure of the transfected RNA fragments and the passage history. Interestingly, in the cross between A59 virus and DIssE RNA, the latter of which lacks the nine-nucleotide sequence CUUUAUAAA, the recombination sites were clustered around the pentanucleotide (UC UAA) repeat, which is located immediately upstream of the nine-nucleotide deletion and at the end of the leader RNA. The role of this nine-nucleotide sequence in replication and recombination is not clear. Curiously, in the cells transfected with a fully replicating DI RNA and infected with a helper virus, the leader sequence of the DI RNAs was readily switched to that of the helper virus only if the DI RNAs contained this nine-nucleotide sequence, suggesting that this nine-nucleotide sequence plays a role in leader switching during DI RNA replication (25). However, these nine nucleotides are not essential for either viral replication or packaging, since some viruses (e.g., MHV-JHM-2c) and naturally occurring DI RNAs with this deletion still have normal replication cycles (25, 27, 28). Nevertheless, in this study, we have observed that the distribution of crossover sites was different for the transfected RNAs with and without this nine-nucleotide sequence (Fig. 3 and 6). It is tempting to suggest that this difference was caused by the presence or absence of this stretch of nucleotides. It is conceivable that, during template-switching, the binding of the nascent RNA transcripts to a new template could generate an unpaired structure caused by the nine-nucleotide deletion, which could force most recombination events to take place near this region. In model A (Fig. 7A), we postulate that the MHV RNA replicase(s) has a proofreading RNase activity, which could remove such a mismatch generated immediately downstream of the UCUAA repeat region and thus create a crossover site in this region. This hypothesis may explain why most recombination sites were confined to the region of UCUAA repeat sequences if the transfected RNAs did not possess the nine-nucleotide sequence.

It is interesting that the clustering of crossover sites changed after serial virus passages, suggesting the selection of certain types of recombinants. This phenomenon has

previously been demonstrated during coinfections with MHVs (3). However, since the number of recombinants examined was not large and some of the minor crossover sites could have been artifacts of the PCR procedure, this interpretation should be viewed with caution. An understanding of the precise structural requirements for RNA recombination and subsequent selection is now feasible with the recombination system described here.

ACKNOWLEDGMENTS

We thank Lisa Welter for editorial assistance.

This work was supported by National Multiple Sclerosis Society grant RG 1449 and Public Health Service research grant AI 19244. M.M.C.L. is an investigator of the Howard Hughes Medical Institute.

REFERENCES

1. **Allison, R., C. Thompson, and P. Ahlquist.** 1990. Regeneration of a functional RNA virus genome by recombination between deletion mutants and requirement for cowpea chlorotic mottle virus 3a and coat genes for systemic infection. Proc. Natl. Acad. Sci. USA **87**:1820–1824.
2. **Baker, S. C., and M. M. C. Lai.** 1991. An in vitro system for the leader-primed transcription of coronavirus mRNAs. EMBO J. **9**:4173–4179.
3. **Banner, L. R., and M. M. C. Lai.** 1991. Random nature of coronavirus RNA recombination in the absence of selection pressure. Virology **185**:441–445.
4. **Baric, R. S., K. Fu, M. C. Schaad, and S. A. Stohlman.** 1990. Establishing a genetic recombination map for murine coronavirus strain A59 complementation groups. Virology **177**:646–656.
5. **Baric, R. S., C.-K. Shieh, S. A. Stohlman, and M. M. C. Lai.** 1987. Analysis of intracellular small RNAs of mouse hepatitis virus: evidence for discontinuous transcription. Virology **156**: 342–354.
6. **Baric, R. S., S. A. Stohlman, M. K. Razavi, and M. M. C. Lai.** 1985. Characterization of leader-related small RNAs in coronavirus-infected cells: further evidence for leader-primed mechanism of transcription. Virus Res. **3**:19–33.
7. **Bujarski, J. J., and A. M. Dzianott.** 1991. Generation and analysis of nonhomologous RNA-RNA recombinants in brome mosaic virus: sequence complementarities at crossover sites. J. Virol. **65**:4153–4159.
8. **Bujarski, J. J., and P. Kaesberg.** 1986. Genetic recombination between RNA components of a multipartite plant virus. Nature (London) **321**:528–531.
9. **Cooper, P. D., A. Steiner-Pryor, P. D. Scotti, and D. Delong.** 1974. On the nature of poliovirus genetic recombinants. J. Gen. Virol. **23**:41–49.
10. **Hirano, N., K. Fujiwara, S. Hino, and M. Matumoto.** 1974. Replication and plaque formation of mouse hepatitis virus (MHV-2) in mouse cell line DBT culture. Arch. Gesamte Virusforsch. **44**:298–302.
11. **Holland, J., K. Spindler, F. Horodyski, E. Grabau, S. Nichol, and S. VandePol.** 1982. Rapid evolution of RNA genomes. Science **215**:1577–1585.
12. **Keck, J. G., G. A. Matsushima, S. Makino, J. O. Fleming, D. M. Vannier, S. A. Stohlman, and M. M. C. Lai.** 1988. In vivo RNA-RNA recombination of coronavirus in mouse brain. J. Virol. **62**:1810–1813.
13. **Keck, J. G., L. H. Soe, S. Makino, S. A. Stohlman, and M. M. C. Lai.** 1988. RNA recombination of murine coronaviruses: recombination between fusion-positive mouse hepatitis virus A59 and fusion-negative mouse hepatitis virus 2. J. Virol. **62**:1989–1998.
14. **Keck, J. G., S. A. Stohlman, L. H. Soe, S. Makino, and M. M. C. Lai.** 1987. Multiple recombination sites at 5′-end of the murine coronavirus RNA. Virology **156**:331–341.
15. **King, A. M. Q., D. McCahon, K. Saunders, J. W. I. Newman, and W. R. Slade.** 1985. Multiple sites of recombination within the RNA genome of foot-and-mouth disease virus. Virus Res. **3**:373–384.
16. **King, A. M. Q., D. McCahon, W. R. Slade, and J. W. I. Newman.** 1982. Recombination in RNA. Cell **29**:921–928.
17. **Kirkegaard, K., and D. Baltimore.** 1986. The mechanism of RNA recombination in poliovirus. Cell **47**:433–443.

17a. **Koetzner, C. A., M. M. Parker, C. S. Richard, L. S. Sturman, and P. S. Masters.** 1992. Repair and mutagenesis of the genome of a deletion mutant of the coronavirus mouse hepatitis virus by targeted RNA recombination. J. Virol. **66**:1841–1848.

18. **Lai, M. M. C.** 1990. Coronavirus: organization, replication and expression of genome. Annu. Rev. Microbiol. **44**:303–333.
19. **Lai, M. M. C.** 1992. RNA recombination in animal and plant viruses. Microbiol. Rev. **56**:61–79.
20. **Lai, M. M. C., R. S. Baric, S. Makino, J. G. Keck, J. Egbert, J. L. Leibowitz, and S. A. Stohlman.** 1985. Recombination between nonsegmented RNA genomes of murine coronavirus. J. Virol. **56**:449–456.
21. **Lai, M. M. C., P. R. Brayton, R. C. Armen, C. D. Patton, C. Pugh, and S. A. Stohlman.** 1981. Mouse hepatitis virus A59: mRNA structure and genetic localization of the sequence divergence from hepatotropic strain MHV-3. J. Virol. **39**:823–834.
22. **Lee, H.-J., C.-K. Shiek, A. E. Gorbalenya, E. V. Koonin, N. La Monica, J. Tuler, A. Bagdzhadzhyan, and M. M. C. Lai.** 1991. The complete sequence (22 kilobases) of murine coronavirus gene 1 encoding the putative proteases and RNA polymerase. Virology **180**:567–582.
23. **Makino, S., N. Fujioka, and K. Fujiwara.** 1985. Structure of the intracellular defective viral RNAs of defective interfering particles of mouse hepatitis virus. J. Virol. **54**:329–336.
24. **Makino, S., J. G. Keck, S. A. Stohlman, and M. M. C. Lai.** 1986. High-frequency RNA recombination of murine coronaviruses. J. Virol. **57**:729–737.
25. **Makino, S., and M. M. C. Lai.** 1989. High-frequency leader sequence switching during coronavirus defective interfering RNA replication. J. Virol. **63**:5285–5292.
26. **Makino, S., C. K. Shieh, J. G. Keck, and M. M. C. Lai.** 1988. Defective-interfering particles of murine coronavirus: mechanism of synthesis of defective viral RNAs. Virology **163**:104–111.
27. **Makino, S., L. H. Soe, C.-K. Shieh, and M. M. C. Lai.** 1988. Discontinuous transcription generates heterogeneity at the leader fusion sites of coronavirus mRNAs. J. Virol. **62**:3870–3873.
28. **Makino, S., F. Taguchi, N. Hirano, and K. Fujiwara.** 1984. Analysis of genomic and intracellular viral RNAs of small plaque mutants of mouse hepatitis virus, JHM strain. Virology **139**:138–151.
29. **Makino, S., K. Yokomori, and M. M. C. Lai.** 1990. Analysis of efficiently packaged defective interfering RNAs of murine coronavirus: localization of a possible RNA-packaging signal. J. Virol. **64**:6045–6053.
30. **Manaker, R. A., C. V. Piczak, A. A. Miller, and M. F. Stanton.** 1961. A hepatitis virus complicating studies with mouse leukemia. J. Natl. Cancer Inst. **27**:29–51.
31. **Meyers, G., N. Tautz, E. J. Dubovi, and H.-J. Thiel.** 1991. Viral cytopathogenicity correlated with integration of ubiquitin-coding sequences. Virology **180**:602–616.
32. **Pachuk, C. J., P. J. Bredenbeek, P. W. Zoltick, W. J. M. Spaan, and S. R. Weiss.** 1989. Molecular cloning of the gene encoding the putative polymerase of mouse hepatitis coronavirus, strain A59. Virology **171**:141–148.
33. **Soe, L. H., C.-K. Shieh, S. C. Baker, M.-F. Chang, and M. M. C. Lai.** 1987. Sequence and translation of the murine coronavirus 5′-end genomic RNA reveals the N-terminal structure of the putative RNA polymerase. J. Virol. **61**:3968–3976.
34. **Steinhauer, D. A., and J. J. Holland.** 1986. Direct method for quantitation of extreme polymerase error frequencies at selected single base sites in viral RNA. J. Virol. **57**:219–228.
35. **Surratt, C. K., S. C. Milan, and M. J. Chamberlin.** 1991. Spontaneous cleavage of RNA in ternary complexes of *Escherichia coli* RNA polymerase and its significance for the mechanism of transcription. Proc. Natl. Acad. Sci. USA **88**:7983–7897.
36. **Weiss, B. G., and S. Schlesinger.** 1991. Recombination between Sindbis virus RNAs. J. Virol. **65**:4017–4025.
37. **Yokomori, K., L. R. Banner, and M. M. C. Lai.** 1991. Heterogeneity of gene expression of the hemagglutinin-esterase (HE) protein of murine coronaviruses. Virology **183**:647–657.